

This is the peer reviewed version of the following article:

Crystal structures of KPC-2 and SHV-1 β -lactamases in complex with the boronic acid transition state analog S02030 / Nguyen, Nhu Q.; Krishnan, Nikhil P.; Rojas, Laura J.; Prati, Fabio; Caselli, Emilia; Romagnoli, Chiara; Bonomo, Robert A.; Van Den Akker, Focco. - In: ANTIMICROBIAL AGENTS AND CHEMOTHERAPY. - ISSN 0066-4804. - 60:3(2016), pp. 1760-1766. [10.1128/AAC.02643-15]

Terms of use:

The terms and conditions for the reuse of this version of the manuscript are specified in the publishing policy. For all terms of use and more information see the publisher's website.

19/12/2025 02:33

**Crystal structures of KPC-2 and SHV-1 β -lactamases in complex with the
boronic acid transition state analog S02030**

Nhu Q. Nguyen^{¶1}, Nikhil P. Krishnan^{¶1}, Laura J. Rojas ², Fabio Prati⁶, Emilia Caselli⁶, Chiara
Romagnoli⁶, Robert A. Bonomo^{1,2,3,4,5}, Focco van den Akker^{1*}

¹ Department of Biochemistry, Case Western Reserve University, 10900 Euclid Ave. Cleveland,
OH 44106, USA

² Research Service, Louis Stokes Cleveland Department of Veterans Affairs Medical Center,
10701 East Boulevard, Cleveland, OH 44106, USA, ³ Department of Medicine,

Case Western Reserve University, Cleveland, OH, USA, ⁴ Department of Pharmacology, Case
Western Reserve University, Cleveland, OH, USA, ⁵ Department of Molecular Biology and
Microbiology, Case Western Reserve University, Cleveland, OH, USA., ⁶Department of Life
Science, University of Modena and Reggio Emilia, Modena, Italy

*Corresponding author.

E-mail: focco.vandenakker@case.edu

[¶]These authors contributed equally.

Abstract

Resistance to expanded-spectrum cephalosporins and carbapenems has rendered certain *Klebsiella pneumoniae* species to be among the most problematic pathogens infecting patients in the hospital and community. This broad spectrum resistance emerges in part via the expression of KPC-2 and SHV-1, and variants thereof, β -lactamases. KPC-2 carbapenemase is particularly worrisome as the genetic determinant encoding this β -lactamase is rapidly spread via plasmids. Moreover, KPC-2, a class A enzyme, is difficult to inhibit with mechanism based inactivators (i.e. clavulanate). In order to develop new β -lactamase inhibitors (BLIs) to add to the limited available armamentarium that can inhibit KPC-2, we have structurally probed the boronic acid transition state analog S02030 for its inhibition of KPC-2 and SHV-1. S02030 contains a boronic acid, a thiophene, and a carboxyl triazole moiety. We present here the 1.54 and 1.87 Å resolution crystal structures of S02030 bound to SHV-1 and KPC-2 β -lactamases, respectively, as well as a comparative analysis of the S02030 binding modes including a previously determined S02030 Class C ADC-7 β -lactamase complex. Upon analysis, S02030 is able to inhibit vastly different serine β -lactamases by interacting with the conserved features of these active sites which includes *i*) forming the bond with catalytic serine via the boron atom, *ii*) positioning of one of the boronic acid oxygens in the oxyanion hole, as well as *iii*) utilizing its amide moiety to make conserved interactions across the width of the active site. In addition, S02030 is able to overcome more distantly located structural differences between the β -lactamases. This unique feature is achieved by reorienting the more polar carboxyl-triazole moiety, generated by click chemistry, to create polar interactions as well as reorient the more hydrophobic thiophene moiety. The former is aided by the unusual polar nature of the triazole ring allowing it to potentially form a unique C-H ...O 2.9Å hydrogen bond with S130 in KPC-2.

43

44 **Introduction**

45 β -lactamases, ubiquitous resistance determinants, provide bacteria with a strong defense against
46 the lethal action of β -lactam antibiotics. *Klebsiella pneumoniae*, an aerobic Gram negative
47 pathogen known to be the agent of serious infections, is capable of expressing numerous β -
48 lactamases including KPC-2 and SHV-1, and variants thereof such as inhibitor resistant and
49 extended spectrum β -lactamases. The KPC-2 β -lactamase is particularly worrisome due to its
50 ability to confer resistance to carbapenems, a class of "last-resort antibiotics", and its rapid
51 dissemination via plasmid transfer not only between but also across species. KPC-2 producing
52 organisms such as *K. pneumoniae*, *Escherichia coli*, and others have caused a number of
53 outbreaks across different continents (1-4). Currently, 24 KPC variants have been identified
54 (lahey.org/Studies), with KPC-2 being the more dominant variant in most countries(5).

55

56 To counteract the presence of β -lactamases, β -lactam antibiotics are often co-
57 administered with a BLI. This successful strategy has significantly prolonged the clinical
58 efficacy of ampicillin, amoxicillin, piperacillin, cefoperazone and ticarcillin (6). Unfortunately,
59 KPC-2 carbapenemase is notoriously difficult to inhibit (7). Currently, there are 4 clinically
60 approved β -lactamase inhibitors with only the most recently FDA approved inhibitor, avibactam,
61 having inhibitory potency against KPC-2 (8). Additional inhibitors, such as the boronic acid
62 containing RPX7009, are in advanced stages of clinical development (as reviewed in (9)). We
63 recently determined the crystal structure of avibactam bound to KPC-2(10). However, having
64 only one potent inhibitor currently available for KPC-2, an enzyme that furthermore has been
65 shown to have the ability to develop avibactam resistance variants (11), suggests that developing
66 additional inhibitors of KPC-2 is warranted to ward off future resistance threats.

67

68 In addition to the currently clinically available set of BLIs that acylate the catalytic
69 serine, a different approach utilizes boronic acid transition state analogs (BATSIs) to inhibit
70 serine β -lactamases such as KPC-2 and SHV-1 (12-14). Such an approach has led to several
71 potent inhibitor compounds (15, 16). Recently, the BATSI S02030 (Fig. 1) was found to inhibit
72 ADC-7 β -lactamase from *Acinetobacter baumannii* by forming a transition state boron-mediated
73 bond with the catalytic serine as observed in the structure of S02030 in complex with ADC-7
74 (17). We now extend the structural investigations of S02030 and observed that it readily inhibits
75 SHV-1 and KPC-2 β -lactamases (see also the companion article Rojas et al(18)). We present
76 here the 1.54 and 1.87 Å resolution crystal structures of S02030 bound to SHV-1 and KPC-2 β -
77 lactamases, respectively, as well as an in depth comparative analyses of the S02030 binding
78 modes including the ADC-7 S02030 complex.

79

80

Materials and Methods

The chemical synthesis of S02030 was previously described (17). The structure of S02030 is represented in Figure 1.

Protein expression, purification, crystallization, and crystal preparation.

The KPC-2 and SHV-1 enzymes were expressed and purified as previously published (10, 13). The KPC-2:S02030 complex was obtained by co-crystallization; the KPC-2 β -lactamase and the S02030 inhibitor were incubated overnight, with a molar ratio of protein:inhibitor of 1:10. Initial co-crystallization screening was carried out using JCSG+ screen kit (from Molecular Dimension) on a 96-well tray (protein was 15mg/ml). The ratio of protein mixture to reservoir was 1:1. The co-crystallization condition was 30% PEG 8000, 0.2 M lithium sulfate, and 0.1 M sodium acetate (pH 4.5). Once KPC-2:S02030 co-crystals grew to their final size, they were mounted and cryoprotected with perfluoropolyether oil (from Hampton Research) prior to flash freezing in liquid nitrogen.

In contrast to KPC-2, the SHV-1:S02030 complex was obtained by soaking the ligand in SHV-1 crystals. Apo SHV-1 crystals were first obtained using 20-30% PEG6000, 100mM Tris pH7.5, and 0.56mM cymal-6 using the vapor diffusion sitting drop crystallization method (19, 20). SHV-1 crystals were soaked for 30min with 5mM S02030 containing mother liquor solution and subsequently cryo-protected in perfluoropolyether oil prior to freezing in liquid nitrogen.

Data Collection and Structure Determination

Data for the KPC-2:S02030 complexes structure was collected on the in-house Rigaku Micromax-007 HF diffraction system. The SHV-1:S02030 data were collected at Stanford Synchrotron Radiation Lightsource (SSRL) beamline 7-1. Both datasets were processed using HKL2000 (21). The S02030 protein complex structures were refined using CCP4 suite program REFMAC(22) and the program COOT(23) was used for model fitting. The initial search models for KPC-2:S02030 complex and SHV-1:S02030 structures were PDB ID 3RXX and 2H5S, respectively. The PRODRG(24) server was used to generate the parameters and topology files for the S02030 ligand that were observed in the Fo-Fc electron density maps in the active site for both β -lactamases (Figs. 2-3). The final coordinates for both S02030 SHV-1 and KPC-2 complex structures were validated using PROCHECK (25) and together with the structure factors were deposited with the Protein Data Bank (PDBid 5EE8 and 5EEC, respectively).

Results and Discussion

We have probed the binding mode of S02030 to two β -lactamases that are common to *K. pneumoniae*, KPC-2 and SHV-1. KPC-2 is clinically the most important carbapenemase(5); our lab has determined its crystal structure as well as its structure in complex with several different inhibitors(10, 13, 26). SHV-1 is part of a large class of over 190 SHV variants some of which some are inhibitor resistance or have an extended-spectrum phenotype. SHV-1 represents a typical class A β -lactamases and its inclusion in this study allows a comparison with both the carbapenemase KPC-2 and the class C ADC-7 β -lactamase; our lab has extensive experience

with obtaining inhibitor complexes with SHV-1 and SHV variants (10, 19, 27-30). The asymmetric unit of the KPC-2:S02030 structure contained two non-crystallographically related molecules A and B. The Fo-Fc difference electron density in the KPC-2 β -lactamase active site of molecule A revealed the presence of a fully occupied S02030 molecule refined with two conformations for the carboxyl-triazole moiety (conformations a and b with occupancies 0.6 and 0.4, respectively; Figs. 2 and 4). S02030 bound to KPC-2 molecule B was less well occupied with an overall occupancy of 0.6; this S02030 molecule adopted a conformation similar to that in molecule A with a b conformation for the carboxyl-triazole moiety (not shown).

The observed S02030 binding modes each have the boron atom of the boronic acid moiety attached to the catalytic S70 residue (Fig. 4). One of the oxygens of the boronic acid moiety occupies the oxyanion hole pocket and the other oxygen occupies the pocket usually known to harbor the deacylation water; the latter pocket is comprised of residues E166 and N170. The amide moiety of S02030 is interacting with both sides of the active site via interactions with the side chain of N132 and the main chain carbonyl of T237 (Fig. 4). The carboxyl-triazole moiety of S02030 interacts, in the a conformation, with S130 via one of the triazole ring nitrogens (N2) involving a 3.1Å hydrogen bond (labeled '1' in Fig. 4). In the b conformation, the carboxyl group of this moiety makes hydrogen bonds with S130 as well as with T235 and T237. Intriguingly, the C5 ring carbon of the triazole moiety in this b conformation is at 2.9Å distance from the O γ of S130 (labeled '2' in Fig. 4) suggesting a C-H...O hydrogen bonding interaction. Such a C-H mediated hydrogen bond is normally unlikely due to its non-polar nature yet in the triazole moiety with its 3 linked nitrogens, the C-H is known to be polar enough to function as a hydrogen bond donor (31, 32). If indeed a C-H mediated hydrogen bond is present, to our knowledge, this would be the first observed C-H...O

hydrogen bond in a triazole-moiety containing ligand with a protein. This could be an important feature to be exploited for future triazole-based drug discovery efforts in particular as this moiety is a key product used in click-chemistry based synthesis efforts(32). In addition to the hydrogen bonds, the carboxyl-triazole moiety in both conformations in molecule A makes π stacking interactions with W105 (Fig. 4); in molecule B, this W105 is repositioned in a different orientation and does not make such an interaction likely due to the lower occupancy of the S02030 in that molecule. Note that, although negatively charged, the carboxyl-triazole moiety also does not make a salt-bridge in either of its two conformations, although there are some electrostatic interactions as K234 and R220 are at 3.8 and 3.9Å distance, respectively, from one of the oxygen atoms of the carboxyl moiety in conformation b. At the other end of S02030, the thiophene moiety makes more limited interactions via a 3.6Å van der Waals interaction with G239.

In the SHV-1 complex structure, S02030 adopts a similar conformation as compared to KPC-2 (Figs. 3 and 5-6). This is exemplified in the boronic acid moiety and amide moieties of S02030 which all make very similar interactions as observed in KPC-2. The carboxyl-triazole moiety adopts a single conformation, unlike what was observed when complexed to KPC-2; this conformation is most similar to that of conformation a in molecule A of the KPC-2 complex structure although overall this moiety is somewhat shifted (Fig. 6). In this SHV-1 complex, the carboxyl-triazole moiety makes a 2.8Å salt-bridge with SHV-1 residue R244 (Fig. 5); this is a difference with the KPC-2 structure as KPC-2 does not have an arginine at this position. An additional difference compared to KPC-2 is that there is no π stacking interaction with residue 105 (Y105 in the case of SHV-1). The thiophene moiety however adopts two conformations in SHV-1 (labeled c and d, Figs. 3 and 5) and is in a different conformation compared to that

observed in KPC-2 (Fig. 6). This thiophene moiety of S02030 is making several van der Waals interactions in the active site of SHV-1 including with carbon atoms of residues N170, T167, and E240. The observation of relatively similar binding modes of S02030 to KPC-2 and SHV-1 is in agreement with the similar IC₅₀ values that were measured for KPC-2 and SHV-1 which are 0.08 and 0.13 μ M, respectively (18). That the affinity of S02030 is nevertheless somewhat higher for KPC-2 could in part be attributed to S02030's ability to have π stacking interactions with a large aromatic residues, W105, in KPC-2 whereas such an interaction is not observed in SHV-1. It is interesting to note that a somewhat similar boronic acid inhibitor, RPX7009, has a similar amide-thiophene moiety yet a different carboxyl containing moiety (33). The RPX7009 structure complexed to a different class A β -lactamase, CTX-M-15, revealed again a similar orientation of the inhibitor generating similar active interactions by its amide-thiophene moieties and carboxyl group (33).

Previously, the structure of S02030 bound to the class C ADC-7 β -lactamase from *A. baumannii* was determined (17) allowing us now to compare the binding mode of S02030 to the two class A β -lactamase determined herein. The ADC-7 S02030 complex structure (PDBid 4U0X) was comprised of 4 independently refined ADC-7 molecules in the asymmetric unit each having a S02030 molecule bound. Analyses of these 4 copies of S02030 bound to ADC-7 showed variability in the positions and orientations of the carboxyl-triazole and thiophene moieties whereas the boronic acid and amide moieties were bound in a similar fashion (17).

Superpositioning of KPC-2 onto one of the ADC-7 S02030 copies reveals interesting differences and similarities (Fig. 7). Key similarities are the presence of the boron bond with the catalytic serine. In addition, the amide moieties provide similar interactions bridging the active

site: the amide nitrogen (labeled “+” in Fig. 7) interacts with the carbonyl oxygen of T237 or the equivalent residue in ADC-7; the amide oxygen (labeled “*”) interacts with N132 or the equivalent N152 in ADC-7 (Fig. 7). An important difference between the S02030 binding modes in KPC-2 and ADC-7 is the orientation of the boronic acid moiety thereby orienting the two boron oxygens in different positions. Notably, Class C β -lactamases do not have a deacylation pocket comprised of E166/N170 thereby forcing the boron oxygen that occupies this pocket in KPC-2 to now reorient itself such that it occupies the oxyanion hole in ADC-7 (both oxyanion hole occupying boron oxygens are labeled “#” in Fig. 7). The other boron oxygen of S02030, the one that occupies the oxyanion hole in KPC-2, has swung away to make space to accommodate the other oxygen in ADC-7. This latter conformational difference is achieved by having a different torsion angle around the C β -O γ bond of the catalytic serine (S70 and S64 in KPC-2 and ADC-7, respectively). The carboxyl-triazole moiety is situated in a somewhat similar position in KPC-2 and ADC-7; the position of the S02030 carboxyl moiety in ADC-7 is closest to that of conformation *a* in KPC-2 although the orientation of triazole ring is flipped (Fig. 7). The thiophene moieties are in the same general vicinity although not identical position. Note that the carboxyl-triazole and thiophene moieties in ADC-7 already showed variability in orientation and position when comparing the 4 independently refined molecules in the ADC-7 structure(17). Note that as previously no IC₅₀ value was determined for S02030 inhibition of ADC-7 (a K_i of 44nM was measured instead (17)) we cannot go into detailed structural comparisons to explain differences in S02030 affinity for ADC-7 as compared to KPC-2 and SHV-1.

Overall, upon comparing the binding modes of S02030 in KPC-2, SHV-1, and ADC-7, a common theme emerges as S02030 is able to recognize and inhibit vastly different serine β -lactamases. Firstly, the S02030 has the ability to interact with the conserved features of these

actives sites and that includes forming the bond with catalytic serine via the boron atom, positioning of one of the boronic acid oxygens in the oxyanion hole, as well as utilizing its amide moiety to make conserved interactions across the width of the active site. Secondly, in regions that are a bit more distant from this very conserved central active site region, S02030 is able to overcome the structural differences between the β -lactamases to maintain its relative broad specificity. These important interactions are achieved by reorienting the more polar carboxyl-triazole moiety to generate polar interactions as well as reorient the more hydrophobic thiophene moiety depending on what active site it is bound in. The polar carboxyl-triazole moiety seems particularly well suited for this former ability as by reorienting and changing its torsions angles, different hydrogen bonds and salt-bridge(s) can be made in different directions depending on the particular active site it needs to bind to; the presence of the carboxyl moiety is well chosen as the β -lactamase active sites are all known to attract and bind carboxyl moiety-containing β -lactam substrates. This remarkable structural plasticity of S02030 is likely key for its ability to recognize related yet different β -lactamases even belonging to different β -lactamase classes.

We recently determined the structure of KPC-2 complexed with avibactam (10). Avibactam is a diazabicyclooctane non- β -lactam BLI. Although avibactam is very different than the BATSI S02030, a comparison between the two inhibitors might elucidate some common features of efficient inhibition of KPC-2. Superpositioning of KPC-2 bound S02030 onto KPC-2 bound avibactam reveals that both inhibitors utilize and occupy the oxyanion hole via an oxygen atom (atoms labeled “#” in Fig. 8). In addition, both avibactam and S02030 have an amide oxygen atom that interacts with residue N132, although the nitrogen atom of this amide in avibactam is not making a direct protein interaction. An additional similarity is that both S02030

and avibactam use a negatively charged moiety to interact with the class A carboxyl recognition pocket (34). This negatively charged inhibitor moiety is a carboxylate in S02030 and a sulfate moiety in avibactam (Fig. 8); each were found to interact with residues T235, T237, and S130 (with R220 and R234 situated at around 4Å distance to provide some electrostatic attraction).

In summary, the S02030 BATSI possesses structural plasticity and can interact efficiently with conserved and variable regions of related β -lactamases. This is in part due to its triazole moiety which is very polar due to the three electronegative nitrogens on one side of the ring; this polar nature allows the carbon on the opposite site of the ring to have the potential to be a unique C-H hydrogen bond donor to complement the already present hydrogen bond acceptor abilities of the ring nitrogens. S02030 utilizes similar features and interactions as a completely different BLI, avibactam to arrive at efficient inhibition of *K. pneumoniae* β -lactamases KPC-2 and SHV-1.

Acknowledgements

Research reported in this publication was supported by the Harrington Foundation, National Institute of Allergy and Infectious Diseases of the National Institutes of Health under Award Numbers R01AI100560 and R01AI063517 to RAB. The content is solely the responsibility of the authors and does not necessarily represent the official views of the National Institutes of Health. This study was also supported in part by funds and/or facilities provided by the Cleveland Department of Veterans Affairs to RAB, the Veterans Affairs Merit Review Program Award 1I01BX001974 to RAB and the Geriatric Research Education and Clinical Center VISN 10 to RAB.

- References**
1. **Silva KE, Cayo R, Carvalhaes CG, Patussi Correia Sacchi F, Rodrigues-Costa F, Ramos da Silva AC, Croda J, Gales AC, Simionatto S.** 2015. Coproduction of KPC-2 and IMP-10 in Carbapenem-Resistant *Serratia marcescens* Isolates from an Outbreak in a Brazilian Teaching Hospital. *J Clin Microbiol* **53**:2324-2328.
 2. **Yu WL, Lee MF, Tang HJ, Chang MC, Walther-Rasmussen J, Chuang YC.** 2015. Emergence of KPC new variants (KPC-16 and KPC-17) and ongoing outbreak in southern Taiwan. *Clin Microbiol Infect* **21**:347 e345-348.
 3. **Bratu S, Landman D, Haag R, Recco R, Eramo A, Alam M, Quale J.** 2005. Rapid spread of carbapenem-resistant *Klebsiella pneumoniae* in New York City: a new threat to our antibiotic armamentarium. *ArchInternMed* **165**:1430-1435.
 4. **Perez F, Endimiani A, Ray AJ, Decker BK, Wallace CJ, Hujer KM, Ecker DJ, Adams MD, Toltzis P, Dul MJ, Windau A, Bajaksouzian S, Jacobs MR, Salata RA, Bonomo RA.** 2010. Carbapenem-resistant *Acinetobacter baumannii* and *Klebsiella pneumoniae* across a hospital system: impact of post-acute care facilities on dissemination. *JAntimicrobChemother* **65**:1807-1818.
 5. **Nordmann P, Poirel L.** 2014. The difficult-to-control spread of carbapenemase producers among Enterobacteriaceae worldwide. *Clin Microbiol Infect* **20**:821-830.
 6. **Drawz SM, Bonomo RA.** 2010. Three decades of β -lactamase inhibitors. *ClinMicrobiolRev* **23**:160-201.
 7. **Watkins RR, Papp-Wallace KM, Drawz SM, Bonomo RA.** 2013. Novel beta-lactamase inhibitors: a therapeutic hope against the scourge of multidrug resistance. *Front Microbiol* **4**:392.
 8. **Ehmann DE, Jahic H, Ross PL, Gu RF, Hu J, Durand-Reville TF, Lahiri S, Thresher J, Livchak S, Gao N, Palmer T, Walkup GK, Fisher SL.** 2013. Kinetics of avibactam inhibition against Class A, C, and D beta-lactamases. *J Biol Chem* **288**:27960-27971.
 9. **Bush K.** 2015. A resurgence of beta-lactamase inhibitor combinations effective against multidrug-resistant Gram-negative pathogens. *Int J Antimicrob Agents* **46**:483-493.
 10. **Krishnan NP, Nguyen NQ, Papp-Wallace KM, Bonomo RA, van den Akker F.** 2015. Inhibition of *Klebsiella* beta-Lactamases (SHV-1 and KPC-2) by Avibactam: A Structural Study. *PLoS One* **10**:e0136813.
 11. **Papp-Wallace KM, Winkler ML, Taracila MA, Bonomo RA.** 2015. Variants of the KPC-2 beta-lactamase which are resistant to inhibition by avibactam. *Antimicrob Agents Chemother* **Epub 9-Feb-2015**.
 12. **Winkler ML, Rodkey EA, Taracila M, Drawz SM, Bethel C, Papp-Wallace K, Smith K, Xu Y, Dwulit-Smith J, Romagnoli C, Caselli E, Prati F, van den Akker F, Bonomo RA.** 2013. Design and exploration of novel boronic acid inhibitors reveals important interactions with a clavulanic acid-resistant sulfhydryl-variable (SHV) β -lactamase. *JMedChem* **56**:1084-1097.
 13. **Ke W, Bethel CR, Papp-Wallace KM, Pagadala SR, Nottingham M, Fernandez D, Buynak JD, Bonomo RA, van den Akker F.** 2012. Crystal structures of KPC-2 β -lactamase in complex with 3-nitrophenyl boronic acid and the penam sulfone PSR-3-226. *AntimicrobAgents Chemother* **56**:2713-2718.
 14. **Ke W, Sampson JM, Ori C, Prati F, Drawz SM, Bethel CR, Bonomo RA, van den Akker F.** 2011. Novel insights into the mode of inhibition of class A SHV-1 β -lactamases revealed by boronic acid transition state inhibitors. *AntimicrobAgents Chemother* **55**:174-183.
 15. **Eidam O, Romagnoli C, Dalmasso G, Barelier S, Caselli E, Bonnet R, Shoichet BK, Prati F.** 2012. Fragment-guided design of subnanomolar beta-lactamase inhibitors active in vivo. *ProcNatlAcadSciUSA* **109**:17448-17453.
 16. **Eidam O, Romagnoli C, Caselli E, Babaoglu K, Pohlhaus DT, Karpiak J, Bonnet R, Shoichet BK, Prati F.** 2010. Design, synthesis, crystal structures, and antimicrobial activity of sulfonamide boronic acids as beta-lactamase inhibitors. *JMedChem* **53**:7852-7863.

17. **Powers RA, Swanson HC, Taracila MA, Florek NW, Romagnoli C, Caselli E, Prati F, Bonomo RA, Wallar BJ.** 2014. Biochemical and Structural Analysis of Inhibitors Targeting the ADC-7 Cephalosporinase of *Acinetobacter baumannii*. *Biochemistry* **53**:7670-7679.
18. **Rojas LJ, Taracila MA, Papp-Wallace KM, Bethel CR, Caselli E, Romagnoli C, Winkler ML, Spellberg B, Prati F, Bonomo RA.** 2015. Boronic acid transition state inhibitors (BATSI)s active against KPC and other class A beta-lactamases: structure activity relationships (SAR) as a guide to inactivator design. *Antimicrob Agents Chemother*.
19. **Padayatti PS, Helfand MS, Totir MA, Carey MP, Hujer HM, Carey PR, Bonomo RA, van den Akker F.** 2004. Tazobactam forms a stoichiometric *trans*-enamine intermediate in the E166A variant of SHV-1 β -lactamase: 1.63 Å crystal structure. *Biochemistry* **43**:843-848.
20. **Kuzin AP, Nukaga M, Nukaga Y, Hujer AM, Bonomo RA, Knox JR.** 1999. Structure of the SHV-1 β -lactamase. *Biochemistry* **38**:5720-5727.
21. **Minor W, Tomchick D, Otwinowski Z.** 2000. Strategies for macromolecular synchrotron crystallography. *Structure* **8**:R105-R110.
22. **Winn MD, Murshudov GN, Papiz MZ.** 2003. Macromolecular TLS refinement in REFMAC at moderate resolutions. *Methods Enzymol* **374**:300-321.
23. **Emsley P, Cowtan K.** 2004. Coot: model-building tools for molecular graphics. *Acta Crystallogr DBiolCrystallogr* **60**:2126-2132.
24. **Schuttelkopf AW, van Aalten DM.** 2004. PRODRG: a tool for high-throughput crystallography of protein-ligand complexes. *Acta Crystallogr DBiolCrystallogr* **60**:1355-1363.
25. **Laskowski RA, MacArthur MW, Moss DS, Thornton JM.** 2001. PROCHECK - a program to check the stereochemical quality of protein structures. *JApplCryst* **26**:283-291.
26. **Ke W, Bethel CR, Thomson JM, Bonomo RA, van den Akker F.** 2007. Crystal structure of KPC-2: insights into carbapenemase activity in class A β -lactamases. *Biochemistry* **46**:5732-5740.
27. **Ke W, Rodkey EA, Sampson JM, Skalweit MJ, Sheri A, Pagadala SR, Nottingham MD, Buynak JD, Bonomo RA, van den AF.** 2012. The importance of the *trans*-enamine intermediate as a β -lactamase inhibition strategy probed in inhibitor-resistant SHV β -lactamase variants. *ChemMedChem* **7**:1002-1008.
28. **Sampson JM, Ke W, Bethel CR, Pagadala SR, Nottingham MD, Bonomo RA, Buynak JD, van den Akker F.** 2011. Ligand-dependent disorder of Ω -loop observed in extended-spectrum SHV-type β -lactamase. *AntimicrobAgents Chemother* **55**:2303-2309.
29. **Totir MA, Padayatti PS, Helfand MS, Carey MP, Bonomo RA, Carey PR, van den Akker F.** 2006. Effect of the Inhibitor-Resistant M69V Substitution on the Structures and Populations of *trans*-Enamine beta-Lactamase Intermediates. *Biochemistry* **45**:11895-11904.
30. **Padayatti PS, Sheri A, Totir MA, Helfand MS, Carey MP, Anderson VE, Carey PR, Bethel CR, Bonomo RA, Buynak JD, van den Akker F.** 2006. Rational design of a β -lactamase inhibitor achieved via stabilization of the *trans*-enamine intermediate: 1.28Å crystal structure of wt SHV-1 complex with a penam sulfone. *JAmChemSoc* **128**:13235-13242.
31. **Kumar A, Pandey PS.** 2008. Anion recognition by 1,2,3-triazolium receptors: application of click chemistry in anion recognition. *Org Lett* **10**:165-168.
32. **Hua Y, Flood AH.** 2010. Click chemistry generates privileged CH hydrogen-bonding triazoles: the latest addition to anion supramolecular chemistry. *Chem Soc Rev* **39**:1262-1271.
33. **Hecker SJ, Reddy KR, Totrov M, Hirst GC, Lomovskaya O, Griffith DC, King P, Tsivkovski R, Sun D, Sabet M, Tarazi Z, Clifton MC, Atkins K, Raymond A, Potts KT, Abendroth J, Boyer SH, Loutit JS, Morgan EE, Durso S, Dudley MN.** 2015. Discovery of a Cyclic Boronic Acid beta-Lactamase Inhibitor (RPX7009) with Utility vs Class A Serine Carbapenemases. *J Med Chem* **58**:3682-3692.

362 34. **Rodkey EA, Drawz SM, Sampson JM, Bethel CR, Bonomo RA, van den Akker F.** 2012. Crystal
363 structure of a pre-acylation complex of the b-lactamase inhibitor sulbactam bound to a
364 sulfenamide bond-containing thiol-beta-lactamase. JAmChemSoc **134**:16798-16804.

365

366

Table 1. X-ray diffraction Data and Refinement Statistics of KPC-2 and SHV-1 S02030 complexes.

	<i>KPC-2 S02030</i>	<i>SHV-1 S02030</i>
<i>Data collection</i>		
Space group	P2 ₁	P2 ₁ 2 ₁ 2 ₁
Unit cell dimensions (Å)	51.85 77.88 64.77 90 108.67 90	49.57 55.19 83.50 90 90 90
Wavelength (Å)	1.5418	1.1271
Resolution (Å)	50-1.85	50-1.54
Redundancy	2.9 (2.3)	3.5 (3.5)
Unique reflections	39,177	33,737
$\langle I \rangle / \langle \sigma(I) \rangle$	9.0 (2.2)	16.5 (2.8)
R_{merge} (%)	10.7 (39.3)	7.0 (42.0)
Completeness (%)	96.7 (90.2)	97.0 (98.3)
<i>Refinement</i>		
Resolution range (Å)	32.9-1.87	33-1.54
R-factor (%)	16.6	14.9
R_{free} (%)	20.1	17.5
RMSD deviation from ideality		
Bond lengths (Å)	0.012	0.012
Angles (deg)	1.72	1.71
<i>Ramachandran plot statistics (%)</i>		
Core regions	93.4	91.3
Allowed regions	6.2	8.2
Additionally allowed regions	0.4	0.4
Disallowed regions	0.0	0.0

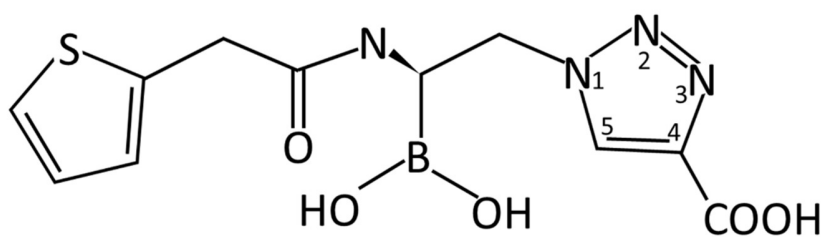


Figure 1. Chemical structure of S02030.

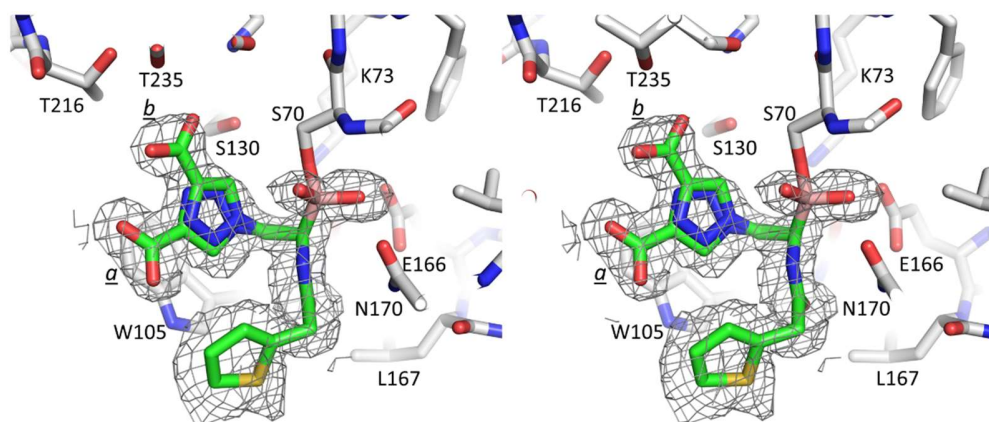


Figure 2. Stereo diagram of difference electron density of active site of KPC-2 β -lactamase showing bound S02030. Alternate conformations of the triazole-carboxylic acid moiety of S02030 are indicated by a/b. Difference density $|F_o|-|F_c|$ map was calculated after 10 rounds of REFMAC refinement with S02030 removed from the refinement and structure factor calculations. Density was contoured at 3σ .

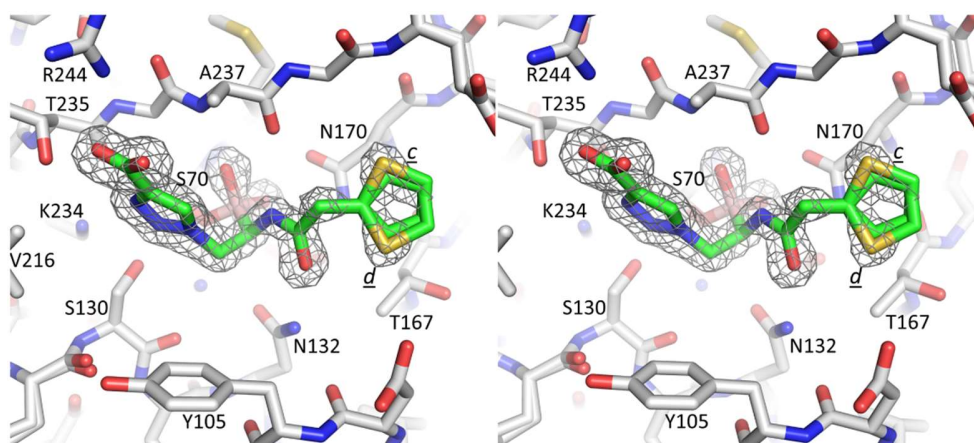


Figure 3. Stereo diagram of difference electron density of active site of SHV-1 showing S02030.

Alternate conformations of the thiophene moiety are indicated by c/d. Map was calculated and contoured as described in Figure 2.

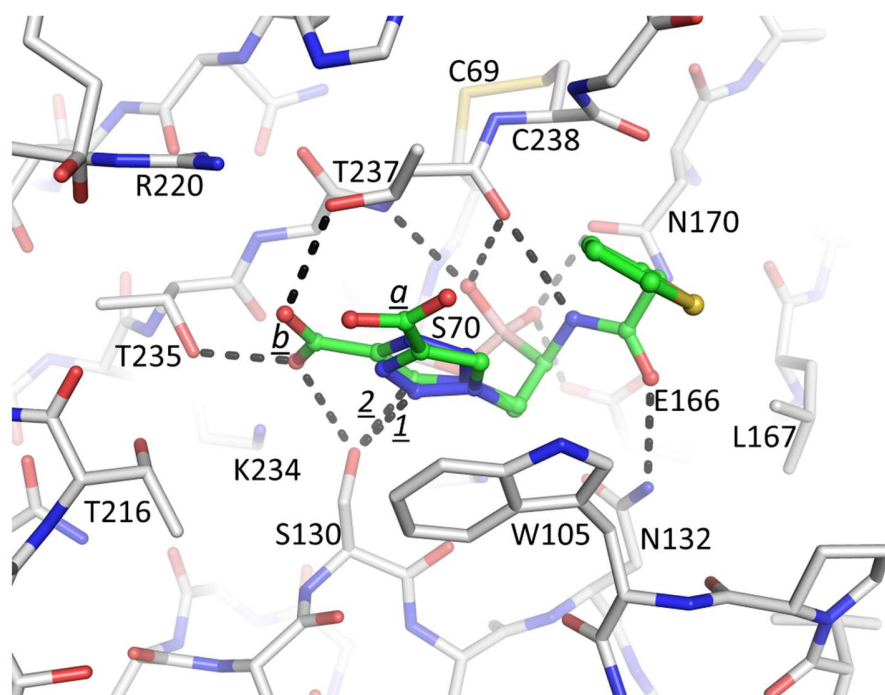


Figure 4. Interactions of S02030 in the active site of KPC-2 β -lactamase. Hydrogen bonds are depicted by dashed lines. The hydrogen bond between the N3 ring nitrogen and S130 in the *a* conformation is labeled as '1'; the C-H...O hydrogen bond between the C5 carbon atom and S130 in the *b* conformation is labeled as '2'.

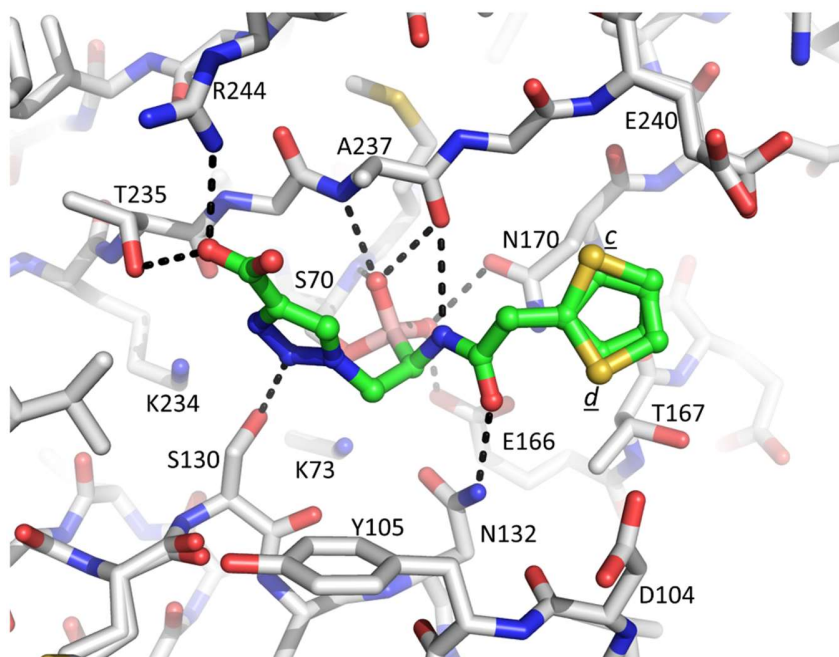


Figure 5. Interactions of S02030 in the active site of SHV-1 β -lactamase.

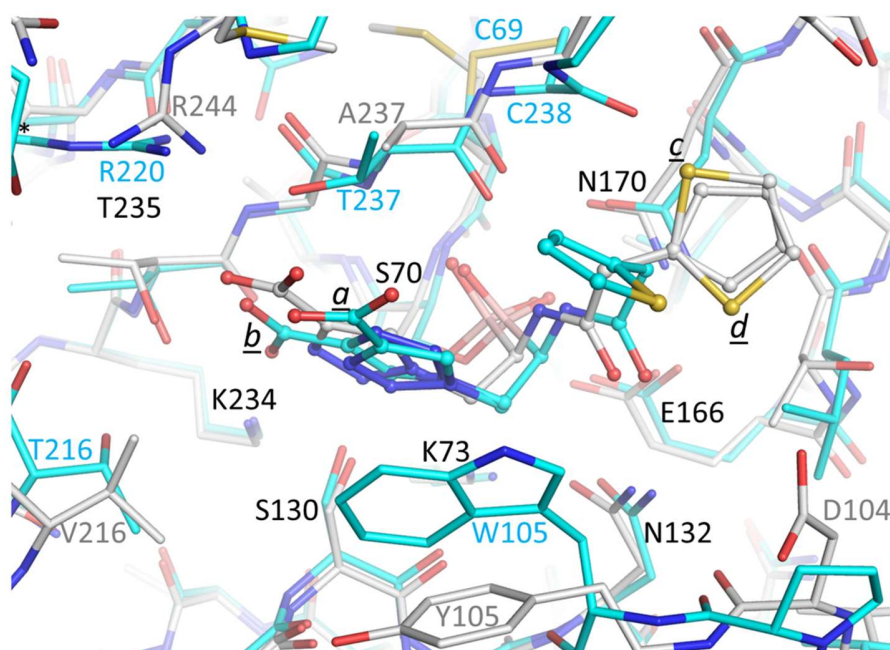


Figure 6. Superposition of SHV-1 and KPC-2 bound S02030 structures. The protein atoms are shown in stick representation and the ligands are shown in ball-and-stick. The KPC-2 S02030 structure is depicted with the carbon atoms in cyan; the SHV-1 S02030 structure with the white carbon atoms. The C α atoms 68-84, 121-140, 167-172, 233-238 of SHV-1 was superimposed on the identical residues of KPC-2 yielding an RMSD of 0.51Å.

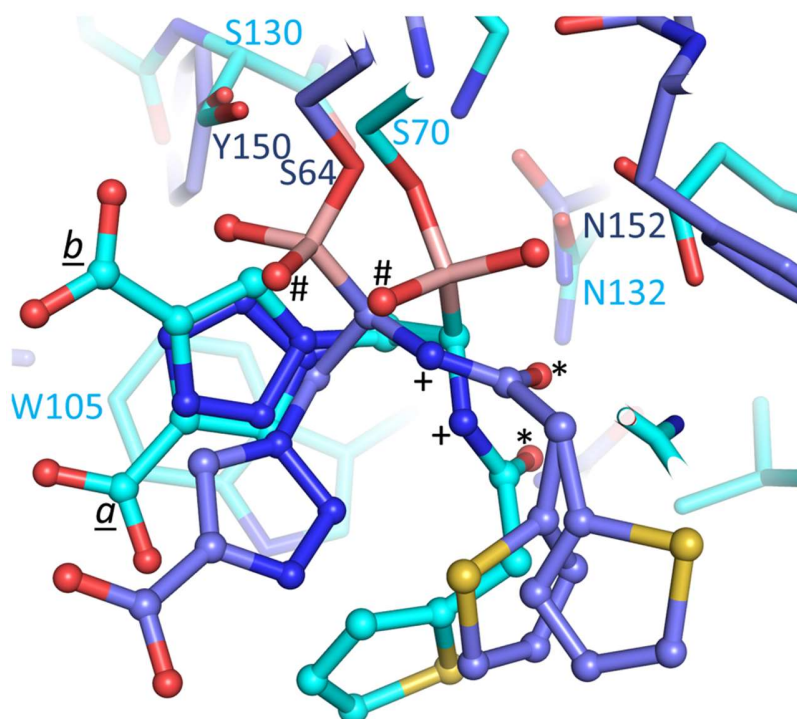


Figure 7. Superposition of ADC-7 and KPC-2 bound S02030 structures. The protein is represented in stick and the inhibitors in ball-and-stick representation; KPC-2 is shown with the cyan colored carbon atoms whereas the ADC-7 carbon coordinates are shown with the medium blue color. The C α atoms of residues 67-84, 132-134, 231-238, 243-249 of KPC-2 were superimposed onto ADC-7 residues 61-78, 152-154, 309-316, 319-325, respectively, with an RMSD of 0.98Å.

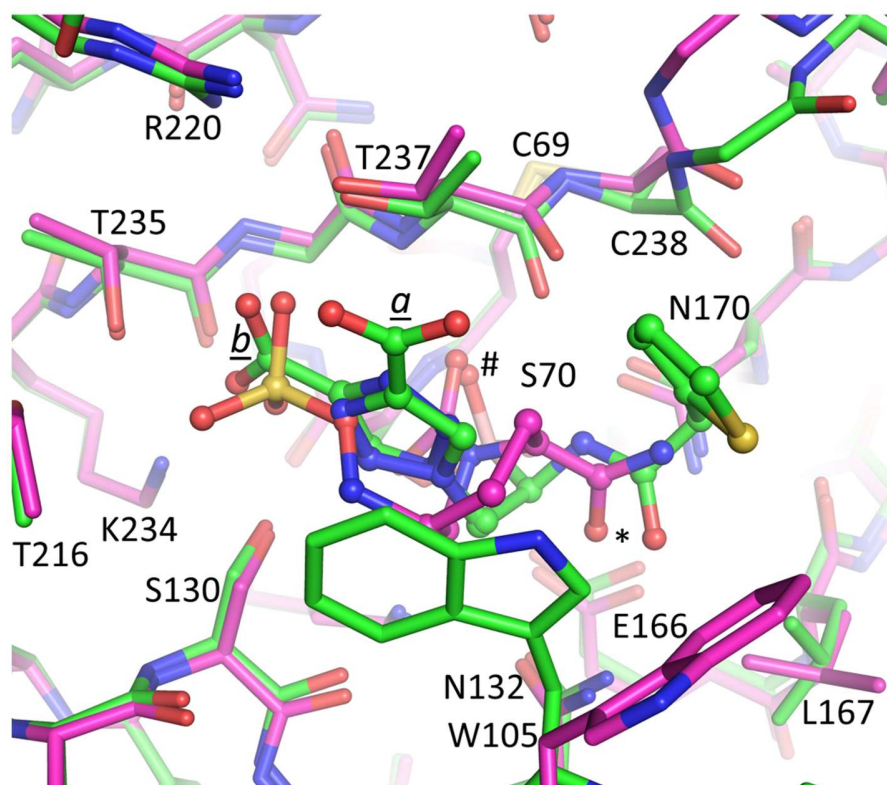


Figure 8. Superposition of S02030 and avibactam bound KPC-2 structures. The protein is in stick representation whereas the inhibitors are in ball-and-stick representation; the KPC-2:S02030 carbon coordinates are in green whereas the KPC-2:avibactam structure has its carbon atoms colored magenta.